

# **Review** of Intra-Beam Scattering (IBS) theory and its application to RHIC

Alexei Fedotov

June 13, 2008

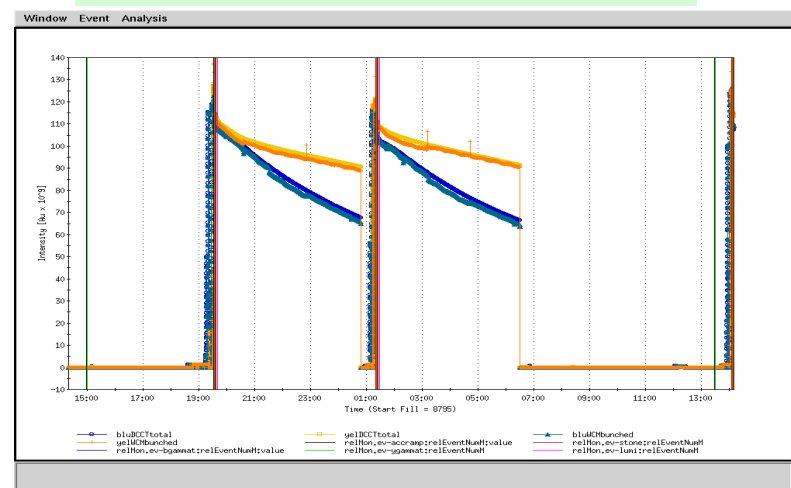
# Outline

2

- A little bit on history of IBS theory
- Basic physics behind
- Application to circular accelerators
- Application to linear accelerators
- IBS scaling and its application to RHIC
- IBS models for RHIC and new developments
- IBS experiments in RHIC and benchmarking with models
- IBS suppression lattice in RHIC

## 2

2007 run  
(with longitudinal stochastic cooling in Yellow ring)



***Performance of the RHIC collider with heavy ions is limited by the process of Intra-Beam Scattering (IBS).***

## What is IBS and what one can do about it?

# What is IBS?

**Intra-Beam Scattering (IBS) – is Multiple Small-angle Coulomb scattering within the beam.**

Charged particle within the beam can scatter via Coulomb collisions.

In general, one should distinguish between

- 1) large-angle single scattering events
- 2) multiple small-angle scattering events

Treatment of both large-angle and small-angle Coulomb collisions is a well known subject from plasma physics.

*The scattering by a relatively large angle in a single encounter is often less likely than a net large angle deflection due to the cumulative effect of many small angle scatterings.*

**In accelerators, both effects were found important:**

- 1) The effect when particles can be **lost as a result of single collision, where energy transfer from horizontal to longitudinal direction is amplified due to relativistic  $\gamma$** , is typically called the **TOUSCHEK effect**.
- 2) When **scattering angles are sufficiently small**, addition at random of **many such collisions** causes beam dimensions to grow (similar to diffusion in gas). The second effect was called by different names, for example, **“Multiple Coulomb scattering”, “Multiple Touscheck effect” and “IBS”**.

# A little bit of history of basic IBS theories

6

In circular accelerators, multiple Coulomb scattering was first applied to explain emittance growth in electron machines:

1. Bruck, Le Duff (1965) – called “multiple Touscheck effect”.

It was later generalized by Piwinski for protons machines, without making any restrictions on beam temperatures.

2. Piwinski (1974) – called “IBS”. Assumed smooth lattice of an accelerator.

The IBS theory was later extended to include variations of the betatron functions and momentum dispersion function along the lattice:

3. Sacherer, Mohl, Hubner & Piwinski (end of 70's) – described in CERN report by Martini (1984).

Another approach for calculation of IBS rates based on the scattering matrix formalism from quantum electrodynamics was used:

4. Bjorken and Mtingwa (1982).

Since then, a variety of models were developed which provide simple approximate results for some regimes of applicability, as well as some refinements of basic theories were done.

# Some refinements of basic theories

7

## Generalization to horizontal-vertical coupled motion:

A. Piwinski

K. Kubo & K. Oide (2001)

V. Lebedev (2004)

## Generalization to relativistic cross section:

Toyomasu (1992)

## Generalizations of B-M to include non-relativistic corrections:

M. Conte & M. Martini (1985)

F. Zimmermann (2006), updated MAD-X

# Basic physics

8

For pure Coulomb collisions, in the center-of-mass system, **classical non-relativistic** differential cross section is given by the Rutherford's formula:

$$\frac{d\sigma}{d\Omega} = \left( \frac{Z_1 Z_2 e^2}{2\mu u^2 \sin^2(\theta/2)} \right)^2$$

For heavy ions within the beam it becomes:

$$\frac{d\sigma}{d\Omega} = \left( \frac{Z^4 e^4}{A^2 m_p^2 u^4} \right) \frac{1}{\sin^4(\theta/2)}$$

In quantum mechanics, collisions of identical particles leads to exchange process which changes cross section:

- 1) non-relativistic case: N. Mott (1930)
- 2) relativistic case: Moller (1932).



For an ion at location  $\mathbf{r}$  with velocity  $\mathbf{v}_1$  colliding with an ion with velocity  $\mathbf{v}_2$  at the same location, the probability rate for scattering into the solid angle  $\Omega$ , averaged over the distribution, is given by:

$$\frac{dP}{dt} = \int d\mathbf{r} \int d\Omega \int d\mathbf{v}_1 f(\mathbf{r}, \mathbf{v}_1) \int d\mathbf{v}_2 f(\mathbf{r}, \mathbf{v}_2) |\mathbf{v}_1 - \mathbf{v}_2| \frac{d\sigma}{d\Omega}$$

One gets basic physics and scaling of the process right away.

What remains is a mathematical formalism to estimate specific quantities of interest.

# Fokker-Planck equation

10

The stochastic interaction of particles where collisions produce only small changes in the velocities of particles is described by the Fokker-Planck equation.

$$\frac{\partial f}{\partial t} + \vec{v} \frac{\partial f}{\partial \vec{r}} + \frac{1}{m} \vec{F} \frac{\partial f}{\partial \vec{v}} = \left( \frac{\partial f}{\partial t} \right)_c$$
$$\left( \frac{\partial f}{\partial t} \right)_c = -\frac{1}{m} \sum_i \frac{\partial}{\partial v_i} (f(\vec{v}) F_i(\vec{v})) + \frac{1}{2} \sum_{ij} \frac{\partial^2}{\partial v_i \partial v_j} (f(\vec{v}) D_{ij}(\vec{v}))$$

Where **F** is the friction force and **D** is diffusion coefficients (functions of  $f(\mathbf{v})$ ).

With this formalism, one has self-consistent description of diffusion process in plasma.

# What is different for charged particle beams in accelerators compared to plasma description?

11

Not much.

Scattering events in beam rest frame are the same.

However, one has to use generalized accelerator coordinates to describe particle motion in accelerator which results in some additional important features:

- 1) **Coupling of longitudinal and transverse (betatron) oscillations** - The curvature of the orbit in circular accelerator produces a **dispersion**. Due to dispersion a sudden change of the energy will always change the betatron amplitudes.
- 2) **“Negative mass” behavior of particles** - Above transition energy, a particle with larger momentum has smaller angular velocity. In other words, when particle is being accelerated it becomes slower and behaves as a particle with negative mass. Because of this, an equilibrium above transition does not exist.

# IBS above and below transition energy

12

The way to appreciate different behavior above and below transition energy is to recall Piwinski's invariant (in smooth approximation):

$$\langle H \rangle \left( \frac{1}{\gamma^2} - \frac{1}{\gamma_t^2} \right) + \frac{\langle \varepsilon_x \rangle}{\beta_x} + \frac{\langle \varepsilon_y \rangle}{\beta_y} = \text{const}$$

where ***H*** is longitudinal invariant of the motion.

- 1) Below transition energy  $\gamma^2 < \gamma_t^2$ , the coefficient in front of ***H*** is positive, i.e. the three amplitudes are limited. The particles can only exchange their oscillation energy. In this case, an equilibrium distribution can exist where IBS does not change the beam dimensions.
- 2) Above transition  $\gamma^2 > \gamma_t^2$ , the coefficient in front of ***H*** is negative. The total oscillation energy can increase. No equilibrium distribution.

# Sketch of typical IBS calculation

13

1. Go to Particle Rest Frame.
2. Assume Rutherford scattering cross section to describe scattering between pairs of identical particles.
3. Compute the change of single-particle emittances in a given binary collision.
4. Assume simple Gaussian phase-space distribution.
5. Average over all collisions (all positions, angles and energy deviations).
6. Write expressions for growth rates of beam dimensions in laboratory frame of reference.

# Piwinski's model (smooth lattice approximation)

14

$$\frac{1}{\tau_p} = \frac{1}{2\sigma_p^2} \frac{d\sigma_p^2}{dt} = nA \frac{\sigma_h^2}{\sigma_p^2} f(a, b, c)$$

$$A = \frac{r_i^2 c N_b}{64\pi^2 \sigma_s \sigma_p \sigma_{x\beta} \sigma_y \sigma_{x'} \sigma_{y'} \beta^3 \gamma^4}$$

$$\frac{1}{\tau_x} = \frac{1}{2\sigma_{x\beta}^2} \frac{d\sigma_{x\beta}^2}{dt} = A \left[ f\left(\frac{1}{a}, \frac{b}{a}, \frac{c}{a}\right) + \frac{D^2 \sigma_p^2}{\sigma_{x\beta}^2} f(a, b, c) \right]$$

$$\frac{1}{\tau_y} = \frac{1}{2\sigma_y^2} \frac{d\sigma_y^2}{dt} = A f\left(\frac{1}{b}, \frac{a}{b}, \frac{c}{b}\right)$$

n=1: bunched beam

n=2: coasting beam

$$p = a^2 + x^2 (1 - a^2)$$

$$q = b^2 + x^2 (1 - b^2)$$

$$f(a, b, c) = 8\pi^2 \int_0^1 \left[ \ln \left( \frac{c^2}{2} \left( \frac{1}{\sqrt{p}} + \frac{1}{\sqrt{q}} \right) \right) - 0.577 \right] (1 - 3x^2) \frac{dx}{\sqrt{pq}}$$

$$a = \frac{\sigma_h}{\gamma \sigma_{x'}} \quad b = \frac{\sigma_h}{\gamma \sigma_{y'}}$$

$$c = \beta \sigma_h \sqrt{2 \frac{\rho_{\max}}{r_i}} \quad \frac{1}{\sigma_h^2} = \frac{1}{\sigma_p^2} + \frac{D^2}{\sigma_{x\beta}^2}$$

# Martini's model (includes lattice derivatives) developed by Sacherer, Mohl, Hubner, Martini & Piwinski <sup>15</sup>

$$\frac{1}{\tau_p} = \left\langle \frac{nA}{2} (1 - d^2) f_1 \right\rangle$$

$$\frac{1}{\tau_{x'}} = \left\langle \frac{A}{2} [f_2 + (d^2 + \tilde{d}^2) f_1] \right\rangle$$

$$\frac{1}{\tau_{z'}} = \left\langle \frac{A}{2} f_3 \right\rangle$$

$$f_i = k_i \int_0^\infty \int_0^\pi \int_0^{2\pi} \sin \mu g_i(\mu, \nu) \exp[-D(\mu, \nu)z] \ln(1 + z^2) d\nu d\mu dz$$

$$D(\mu, \nu) = \frac{[\sin^2 \mu \cos^2 \nu + \sin^2 \mu (a \sin \nu - \tilde{d} \cos \nu)^2 + b^2 \cos^2 \mu]}{c^2}$$

$$g_1(\mu, \nu) = 1 - 3 \sin^2 \mu \cos^2 \nu$$

$$g_2(\mu, \nu) = 1 - 3 \sin^2 \mu \sin^2 \nu + 6 \tilde{d} \sin \mu \sin \nu \cos \nu / a$$

$$g_3(\mu, \nu) = 1 - 3 \cos^2 \mu$$

$$d = \frac{\sigma_p}{\sigma_x} D \quad \tilde{d} = \frac{\sigma_p}{\sigma_x} \tilde{D} \quad a = \frac{\sigma_y}{\sigma_{x\beta}} \sqrt{1 + \alpha_x^2} \quad b = \frac{\sigma_y}{\sigma_{z'}} \quad c = q \sigma_y \quad k_1 = 1/c^2, \quad k_2 = a^2/c^2, \quad k_3 = b^2/c^2,$$

# Bjorken & Mtingwa model (with extension to include vertical dispersion, Venturini'2001)

16

$$\left\{ \begin{aligned} \frac{1}{\tau_x} &= \left\langle \frac{H_x}{\epsilon_x} \gamma_0^2 I_{zz} - 2 \frac{\beta_x \phi_{Bx}}{\epsilon_x} \gamma_0 I_{xz} + \frac{\beta_x}{\epsilon_x} I_{xx} \right\rangle_s \\ \frac{1}{\tau_y} &= \left\langle \frac{H_y}{\epsilon_y} \gamma_0^2 I_{zz} - 2 \frac{\beta_y \phi_{By}}{\epsilon_y} \gamma_0 I_{yz} + \frac{\beta_y}{\epsilon_y} I_{yy} \right\rangle_s \\ \frac{1}{\tau_z} &= \left\langle \frac{1}{2} \frac{\gamma_0^2}{\sigma_p^2} I_{zz} \right\rangle_s \end{aligned} \right.$$

$$H_i = \beta_i D_i'^2 + 2\alpha_i D_i D_i' + \gamma D_i^2$$

$$\phi_{Bi} = D_i' + \alpha_i D_i / \beta_i$$

$$A = \frac{c r_i^2 N L_c}{8\pi \beta^3 \gamma_0^2 \epsilon_x \epsilon_y \sigma_p \sigma_s}$$

$$I_{ij} = A \int_0^\infty d\lambda \frac{\lambda^{1/2}}{\sqrt{\det \Lambda}} (\delta_{ij} \text{Tr} \Lambda^{-1} - 3 \Lambda_{ij}^{-1})$$

$$\Lambda = I\lambda + L$$

$$L = \begin{bmatrix} \frac{\beta_x}{\epsilon_x} & 0 & -\gamma_0 \frac{\beta_x \phi_{Bx}}{\epsilon_x} \\ 0 & \frac{\beta_y}{\epsilon_y} & -\gamma_0 \frac{\beta_y \phi_{By}}{\epsilon_y} \\ -\gamma_0 \frac{\beta_x \phi_{Bx}}{\epsilon_x} & -\gamma_0 \frac{\beta_y \phi_{By}}{\epsilon_y} & \frac{\gamma_0^2 H_x}{\epsilon_x} + \frac{\gamma_0^2 H_y}{\epsilon_y} + \frac{\gamma_0^2}{\sigma_p^2} \end{bmatrix}$$



# Approximate formulas

17

Accurate IBS models: Bjorken-Mtingwa or Martini (modified Piwinski) require some computational time – formulas has to be evaluated at each element of the lattice along the ring.

As a result, many different approximate models, which are much easier to use, were constructed.

The most known at RHIC are high-energy approximations by

1. G. Parzen

2. J. Wei

# Simple scaling from first principles

18

Simple scaling can be obtained from first principles in some limiting cases.

From diffusion coefficient (gas-relaxation formula)

1.  $\tau^{-1} = \frac{4\pi n(Ze)^4}{m^2} \frac{\Lambda}{\Delta^3}$  For isotropic Maxwellian distribution,  
where  $\Delta$  is rms velocity spread, and  $\Lambda$  is Coulomb logarithm.

2. For flattened velocity distribution when longitudinal velocity spread in beam rest frame is much smaller than transverse (typical for high energies in accelerator).

$$\tau_{\parallel}^{-1} = \frac{1}{\Delta_{\parallel}^2} \frac{d\bar{v}_z^2}{dt} = 4\pi m(Ze)^4 \mu \Lambda \frac{\Delta_{\perp}}{\Delta_{\parallel}}$$

$$f(\vec{r}, \vec{v}) = \frac{n}{\pi \sqrt{\pi} \Delta_{\perp}^2 \Delta_{\parallel}} e^{-(v_x^2 + v_y^2)/\Delta_{\perp}^2} e^{-v_z^2/(2\Delta_{\parallel}^2)}$$

$$\tau_{\parallel}^{-1} = \frac{1}{\sigma_p^2} \frac{d\sigma_p^2}{dt} = \frac{r_i^2 c N_i \Lambda}{8\beta^3 \gamma^3 \epsilon_x^{3/2} \langle \beta_{\perp}^{1/2} \rangle \sqrt{\pi/2} \sigma_s \sigma_p^2}$$

Fedotov, 2004

$$\tau_{\perp}^{-1} = \frac{\sigma_p^2}{\epsilon_x} \left\langle \frac{D_x^2 + (D_x' \beta_x + \alpha_x D_x)^2}{\beta_x} \right\rangle \tau_{\parallel}^{-1}$$

$$\tau_{\parallel}^{-1} = \frac{r_i^2 c N_i \Lambda}{8\beta^3 \gamma^3 \epsilon_x^{3/2} \langle \beta_{\perp}^{1/2} \rangle \sigma_s \sigma_p^2}$$

Bjorken-Mtingwa  
high-energy approximation

# Simple scaling (high-energy, $\gamma \gg \gamma_t$ )

19

IBS is dominated by longitudinal diffusion:

$$\tau_{\parallel}^{-1} = \frac{1}{\sigma_p^2} \frac{d\sigma_p^2}{dt} = \frac{r_i^2 c N_i \Lambda}{8 \beta^3 \gamma^3 \epsilon_x^{3/2} \langle \beta_{\perp}^{1/2} \rangle \sqrt{\pi / 2} \sigma_s \sigma_p^2}$$

Because of dispersion, longitudinal diffusion is transferred into transverse direction also:

$$\tau_{\perp}^{-1} = \frac{\sigma_p^2}{\epsilon_x} \left\langle \frac{D_x^2 + (D_x' \beta_x + \alpha_x D_x)^2}{\beta_x} \right\rangle \tau_{\parallel}^{-1}$$

$$IBS \rightarrow \frac{Z^4}{A^2 m^2} \frac{N_i}{\epsilon_{xN}^{3/2} \sigma_s}$$

- more important for heavy ions than protons due to  $Z^4/A^2$
- more important for electrons than protons due to  $m^2$
- becomes more important for higher beam densities

$$g_f = \left( \frac{\Delta_{\parallel}}{\Delta_{\perp}} \right)^2 = \frac{\langle \beta_{\perp} \rangle \sigma_p^2}{\gamma^2 \epsilon_{\perp}}$$

Applicability of high-energy approximation is when  $g_f^{1/2} \ll 1$

# Below transition energy

20

Behavior is similar to gas-relaxation:

in beam frame:

$$\tau^{-1} = \frac{4\pi n(Ze)^4}{m^2} \frac{\Lambda}{\Delta^3}$$

Relaxation towards equilibrium is possible in smooth approximation

in lab frame:

$$\tau^{-1} = \frac{\mu 4\pi (Ze)^4 m \Lambda}{\gamma}$$

where  $\mu$  is phase-space density and  $\Lambda$  is Coulomb logarithm.

# IBS in linear accelerators

21

(As an example: estimate by Gluckstern & Fedotov, 1999)

Motivated by studies of halo formation in high-intensity proton linacs

(Note: not a relaxation effect such as the Boersch effect which is relaxation due to Coulomb collisions in strongly anisotropic beams).

Both single and multiple scattering was estimated:

$$\frac{dP}{dt} = \int dr \int d\Omega \int dv_1 f(r, v_1) \int dv_2 f(r, v_2) |v_1 - v_2| \frac{d\sigma}{d\Omega}$$

$$f(r, \mathbf{v}) = \begin{cases} N(H_0 - H)^n = N[G(r) - mv^2/2]^n, & H < H_0, \\ 0, & H > H_0, \end{cases}$$

$$H(r, \mathbf{v}) = mv^2/2 + kr^2/2 + e\Phi_{sc}(r)$$

11-dimensional  
integral was evaluated  
analytically for a variety  
of distribution function  
(from singular to Maxwellian)

Large-angle  
single scattering  
results

$$\frac{dP}{cdt} \sim \begin{cases} r_p^2/\epsilon_N^3, & n > 0, \\ (r_p^2/\epsilon_N^3) \ln(\epsilon_N^2/r_p a), & n = 0, \\ (r_p^2/\epsilon_N^3) (\epsilon_N^2/r_p a)^{-n}, & 0 < -n < 1 \end{cases}$$

Multiple  
small-angle  
Scattering  
result

$$\frac{dP}{cdt} \sim \frac{r_p^2}{\epsilon_N^3} \ln\left(\frac{1}{\theta_D}\right)$$

- IBS effect was found negligible for proton accelerators
- However, it may become important for electron linacs with high phase-space density like ERL's (Fedotov, ERL05).

# Limitations of IBS models

22

In some recent IBS reviews it is stated that there are

**two major limitations in IBS theories:**

1. The use of non-relativistic scattering cross section.
2. The use of Gaussian beam distribution to construct expressions for growth rates.

Actually,

1. Generalization to relativistic cross section was done quite some time ago (Toyomasu, 1992).
2. IBS formalism for arbitrary distributions in 3-D was implemented in BETACOOOL code (2007).

# IBS treatments for non-Gaussian distributions 23

To simulate spreading of non-Gaussian longitudinal beam profiles and loss from RF bucket **1-D Fokker-Plank** solvers were used successfully:

For example:

1. J. Wei et al. (BNL)

2. V. Lebedev et al. (FNAL)

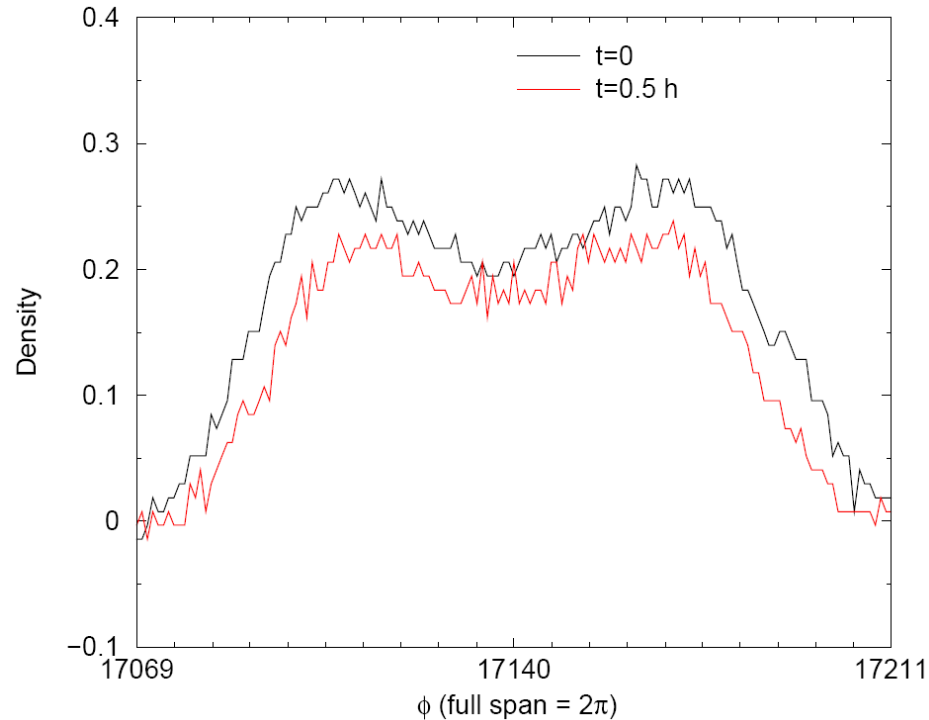
- For initial distribution close to Gaussian and IBS diffusion – not a big difference compared to Gaussian approximation.
- However, such treatment becomes essential for distributions which strongly differ from a Gaussian.

# Evolution of hollow longitudinal beam profile

(J. Wei, A. Fedotov, W. Fischer, N. Malitsky, G. Parzen, J. Qiang, HB2004) <sup>24</sup>

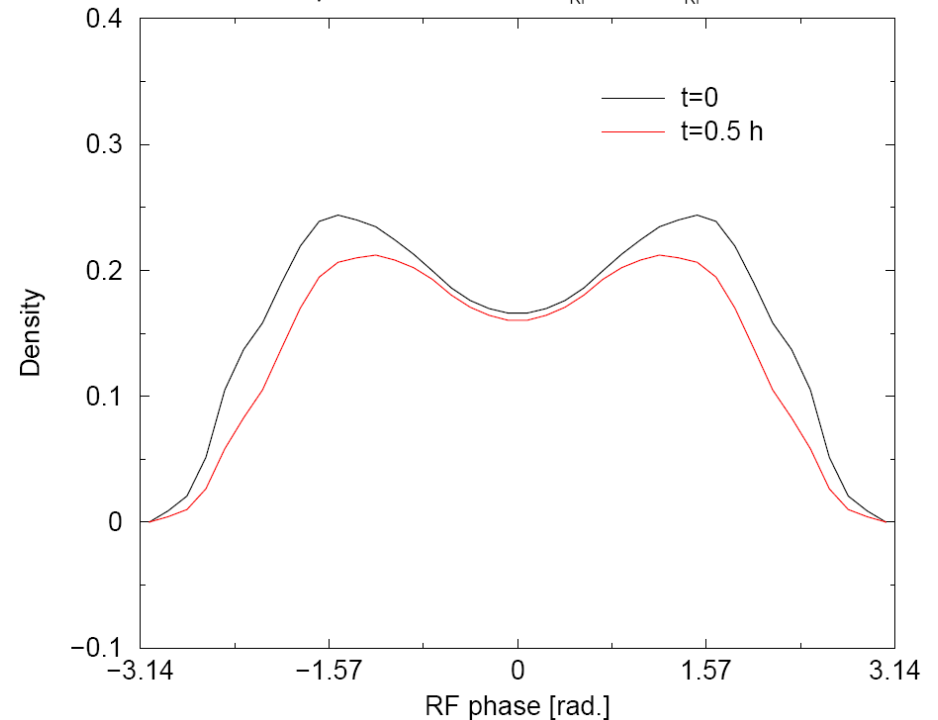
RHIC WCM 2004-3-16 run #4790 Yellow

trace 1079495460 and 1079497224, bunch #3



BBFP 2004-3-16 #4790 Blue

Au beam,  $\gamma=108$ ,  $N=0.55 \times 10^9$ ,  $h_{RF}=360$ ,  $V_{RF}=300$  kV

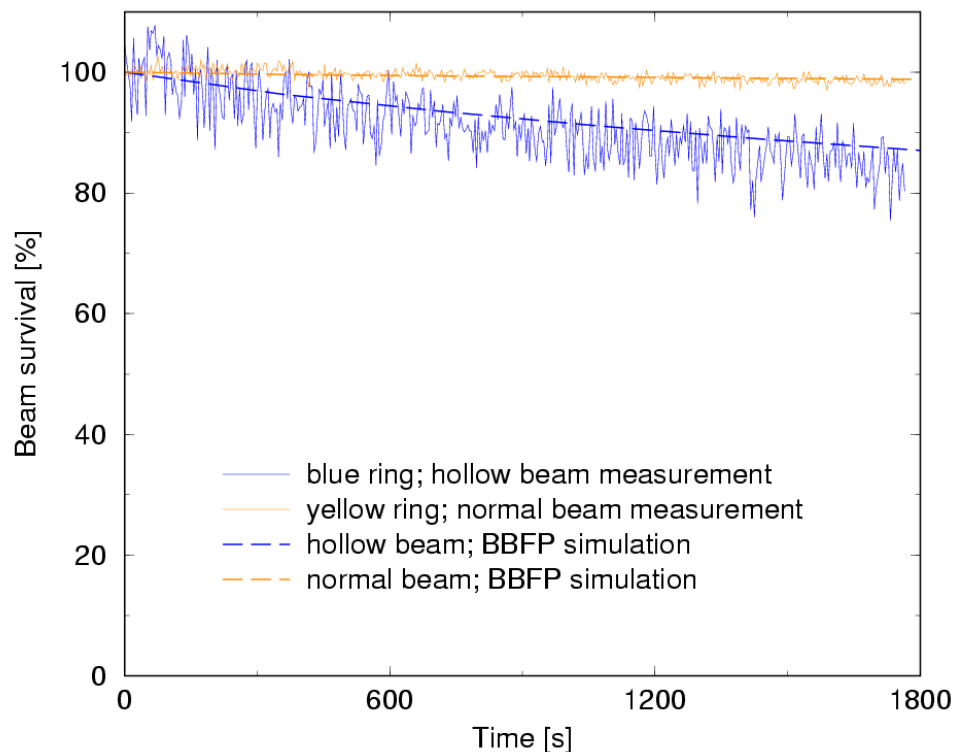




# Beam de-bunching loss benchmarking

(J. Wei, A. Fedotov, W. Fischer, N. Malitsky, G. Parzen, J. Qiang, HB2004) <sup>25</sup>

WCM measurement vs. BBFP code simulation by J. Wei (2004).



1) Typical, close to Gaussian, longitudinal profile in Yellow ring.

2) Hollow longitudinal beam profile in Blue ring.

# Implementation and development of IBS models for RHIC

26

To have an accurate design of high-energy electron cooler for RHIC, it was necessary to have accurate description of IBS process in RHIC:

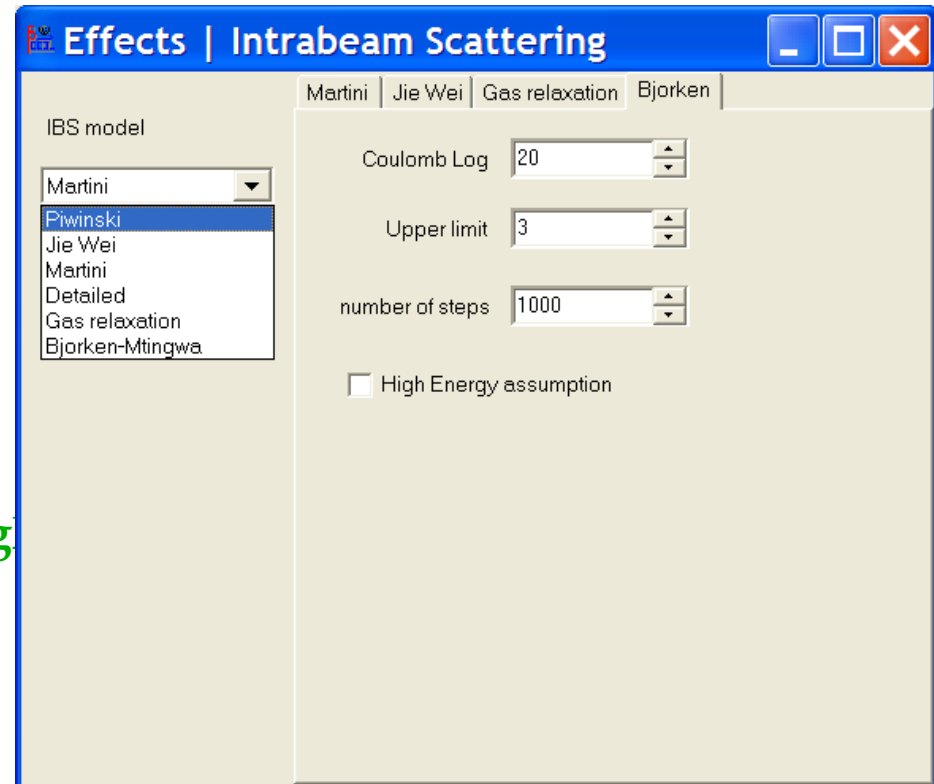
1. Various IBS models were implemented in BETACOOOL code.
2. Models were benchmarked with one another.
3. IBS calculation within BETACOOOL was benchmarked with other codes.
4. Dedicated measurements of IBS in RHIC were performed and compared to models.

# IBS models in BETACOOOL code (JINR, Dubna, Russia) <sup>27</sup>

## - Gaussian distributions

### I. Analytic models for Gaussian distribution:

- Piwinski's model
- Martini's model (including derivatives of lattice functions)
- Bjorken-Mtingwa's model (including vertical dispersion)
- Wei's, Parzen's models (high energy approximation)
- Gas-relaxation model (high-energy approximation)



# IBS models in BETACOOOL – non-Gaussian distributions

28

## II. IBS for non-Gaussian distributions.

In situations when distribution can strongly deviate from Gaussian, as for example under effect of Electron Cooling, it was necessary to develop IBS models based on the amplitude dependent diffusion coefficients.

Several models were developed:

- “Detailed” (Burov): analytic expression for longitudinal coefficient for Gaussian distribution with longitudinal temperature much smaller than transverse and smooth lattice approximation.
- “bi-Gaussian” (Parzen): rms rates for bi-Gaussian distribution; all particles are kicked based on the rms rate expression.
- “Core-tail”: different diffusion coefficients for particle in the core and tails of the distribution.
- “Kinetic model”
- “Local diffusion” – algorithm is based for numerical evaluation of amplitude dependent diffusion coefficients in 3-D. Allows to simulate evolution of arbitrary distribution due to IBS.

## 3-D IBS model for non-Gaussian distribution (numerical evaluation of amplitude dependent diffusion coefficients)

29

After extensive development, the model was finally implemented in BETACOOOL code in 2007 (A. Sidorin, A. Smirnov et al., BNL-BETACOOOL report December 2007).

$$\vec{F} = \frac{\langle \Delta \vec{p} \rangle}{\Delta t} = - \frac{4\pi n e^4 Z_t^2 Z_f^2}{\left( \frac{m_f m_t}{m_f + m_t} \right)} \int \ln \left( \frac{\rho_{\max}}{\rho_{\min}} \right) \frac{\vec{U}}{U^3} f(v) d^3 v \quad \begin{pmatrix} D_{x,x} & D_{x,y} & D_{x,z} \\ D_{x,y} & D_{y,y} & D_{y,z} \\ D_{x,z} & D_{y,z} & D_{z,z} \end{pmatrix}$$

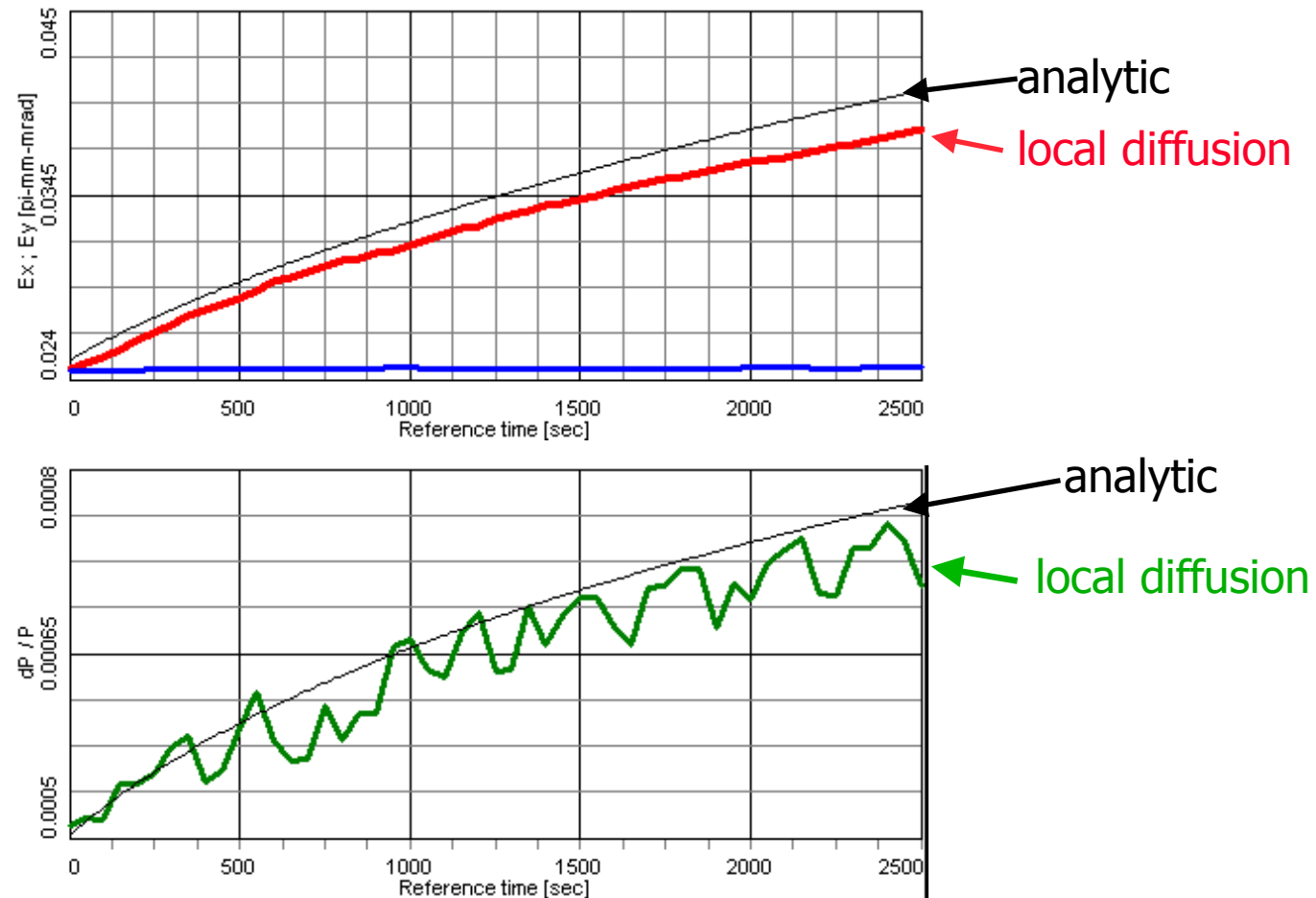
$$D_{\alpha,\beta} = \frac{\langle \Delta p_\alpha \Delta p_\beta \rangle}{\Delta t} = 4\pi n e^4 Z_t^2 Z_f^2 \int \ln \left( \frac{\rho_{\max}}{\rho_{\min}} \right) \frac{U^2 \delta_{\alpha,\beta} - U_\alpha U_\beta}{U^3} f(v) dv$$

Mathematical formulation of implemented expressions is quite involved but they were implemented and benchmarked vs. some limiting cases.

This model of IBS is called "Local diffusion" in BETACOOOL code.

# Simulation comparison of “Local diffusion” vs. analytic model for Gaussian distribution (A. Sidorin, 2007)

30



# Dedicated measurements of IBS in RHIC

31

1. To ensure accurate benchmarking, collisions were turned off. In addition,  $h=360$  rf system was used to avoid loss of particles from the bucket.
2. Six bunches of different intensity with different initial emittance were injected, which allowed us to test expected scaling with intensity and emittance.
3. Measurements of the bunch length were done using Wall Current Monitor (WCM).
4. Measurements of the horizontal and vertical emittance in each individual bunch were done using Ionization Profile Monitor (IPM).

2004 – with Au ions

2005 – with Cu ions

2007 – Au ions with IBS-suppression lattice

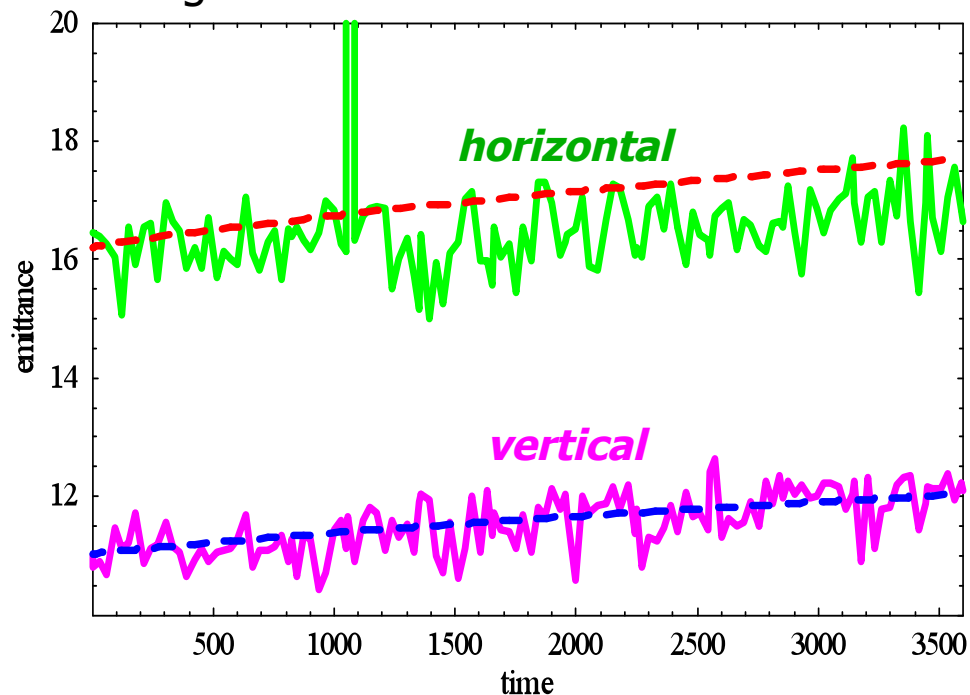
2008 – Au ions with operational IBS-suppression lattice

# IBS in RHIC – measurements vs theory

## Example of 2005 data with Cu ions.

32

Simulations (BETACOOOL) – Martini's model of IBS for exact designed lattice of RHIC, including derivatives of the lattice functions.



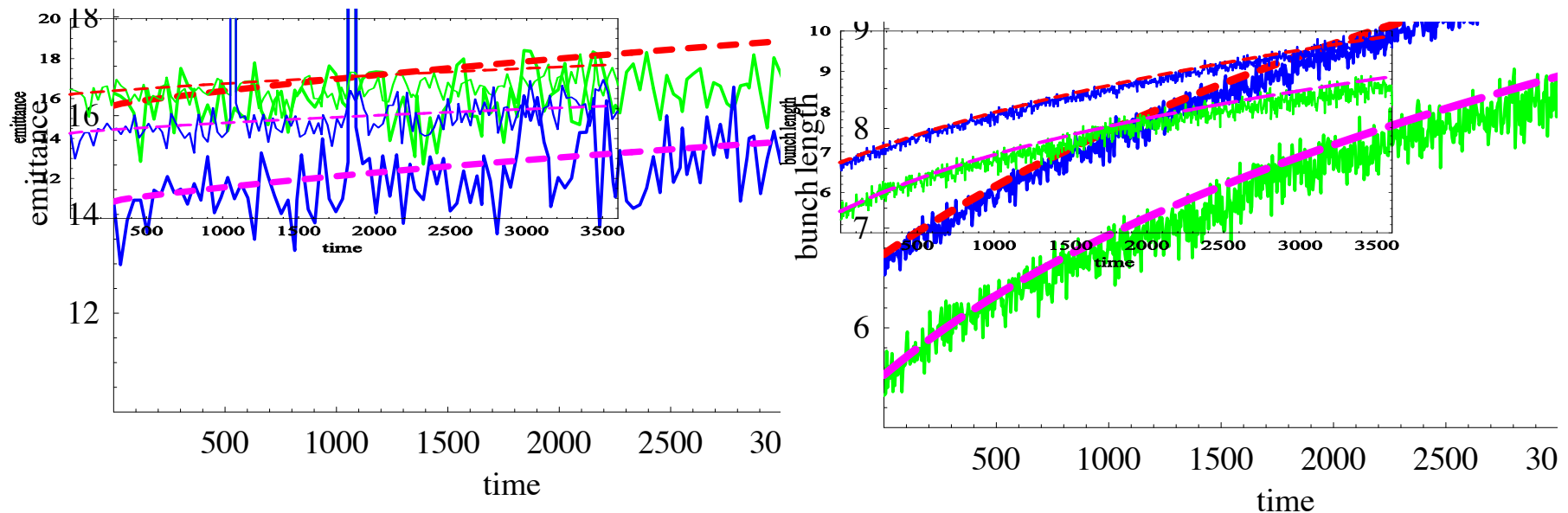
Growth of 95% normalized emittance [ $\mu\text{m}$ ]  
for bunch with intensity  $N=2.9 \cdot 10^9$



# Simulations vs. Measurements (Cu ions, APEX 2005)

33

Two bunches with different intensity.



Growth of 95% normalized horizontal emittance [ $\mu\text{m}$ ] for two bunch intensities  $N = 2.9 \cdot 10^9$  (upper curve) and  $1.4 \cdot 10^9$ . Dash lines - simulations; solid lines - measurements.

FWHM [ns] bunch length growth for intensities  $N = 2.9 \cdot 10^9$  and  $1.4 \cdot 10^9$ .

# IBS in RHIC (for $\gamma \gg \gamma_{tr}$ ) & IBS suppression lattice

34

1. For energies much higher than transition energy Intra-beam Coulomb scattering (IBS) is dominated by heating of longitudinal degree of freedom.

$$\tau_{\parallel}^{-1} = \frac{r_i^2 c N_i \Lambda}{8 \beta^3 \gamma^3 \epsilon_x^{3/2} \langle \beta_{\perp}^{1/2} \rangle \sigma_s \sigma_p^2}.$$

Additional heating:

2. At regions with non-zero dispersion, changes in longitudinal momentum change particle reference orbits, which additionally excites horizontal betatron motion.

$$\tau_{\perp}^{-1} = \frac{\sigma_p^2}{\epsilon_x} \left( \frac{D_x^2 + (D'_x \beta_x + \alpha_x D_x)^2}{\beta_x} \right) \tau_{\parallel}^{-1},$$

3. Horizontal heating is shared between horizontal and vertical planes due to x-y coupling. For the case of full coupling, transverse heating is equally shared between x and y.

$$H = \gamma_x D_x^2 + 2\alpha_x D_x D'_x + \beta_x D_x'^2$$

Reducing this function allows to reduce transverse IBS rate – idea behind “IBS-suppression” lattice.

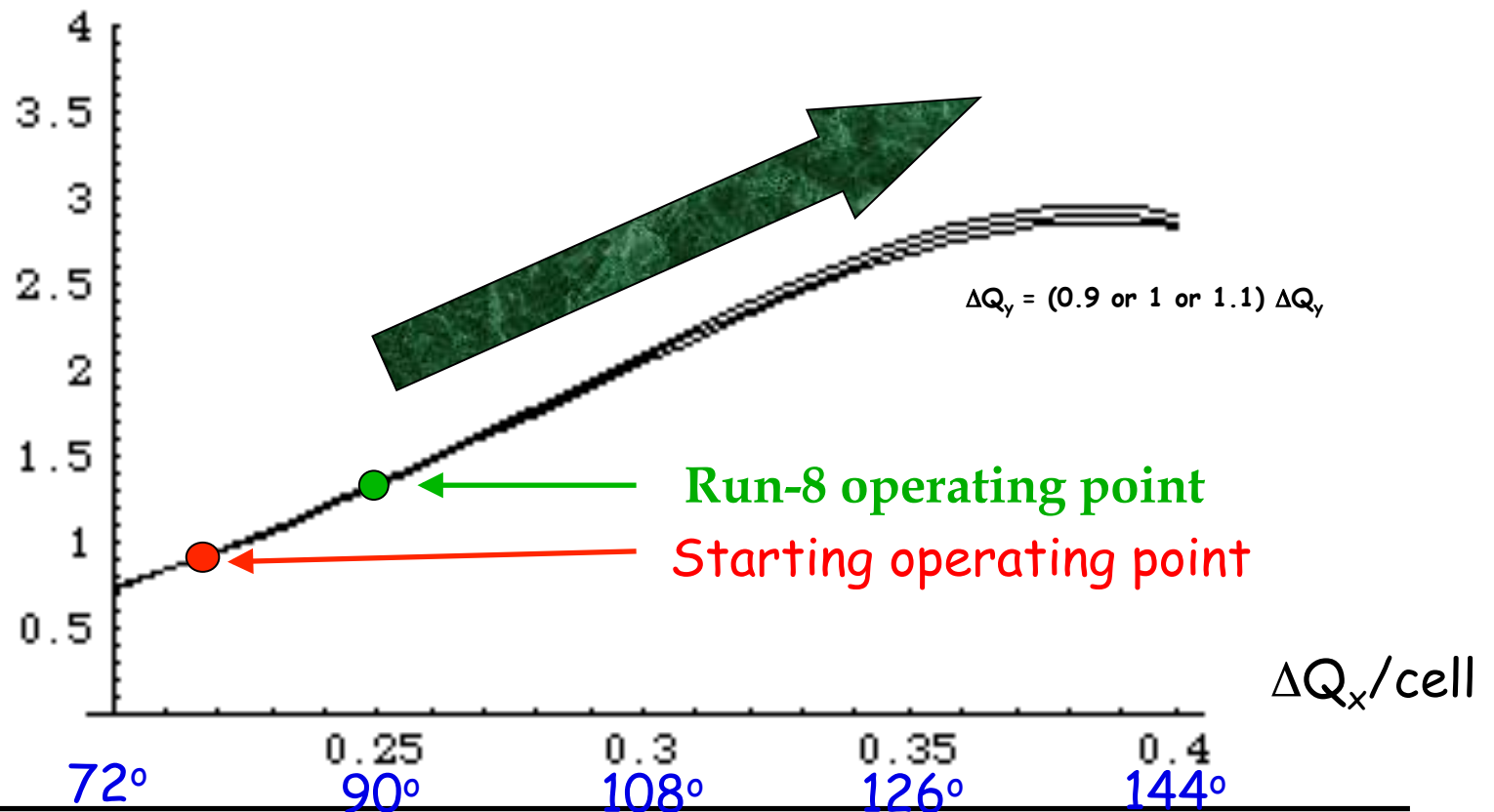
## Reduction of the IBS rate

V.N. Litvinenko

35

$$\text{IBS}(0.22) / \text{IBS}(\Delta Q_x)$$

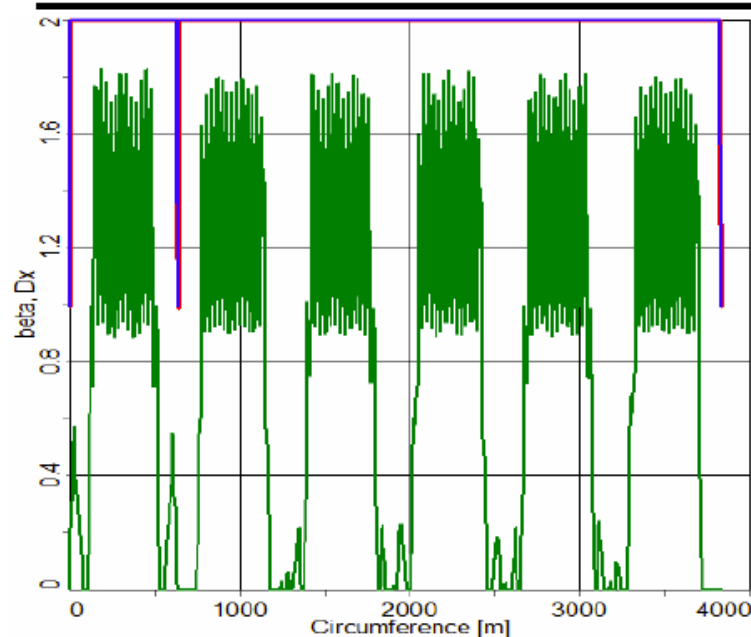
NOTE:  $\Delta Q_x$  are tune advances per FODO cell



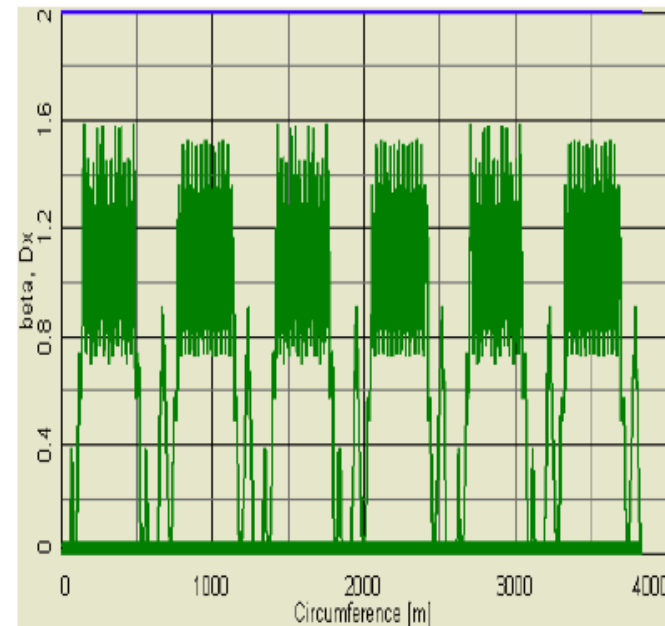
## Test lattice for IBS reduction (for APEX experiments)

RHIC-4 lattice vs 92 degree phase advance

36



RHIC-4 dispersion



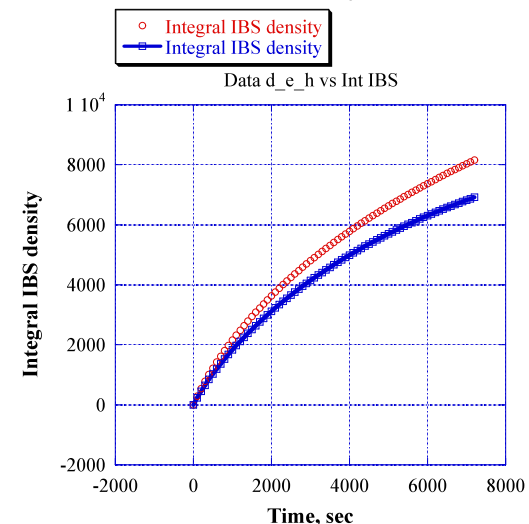
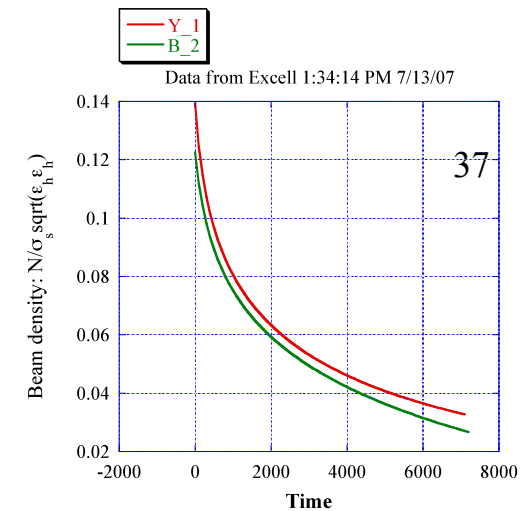
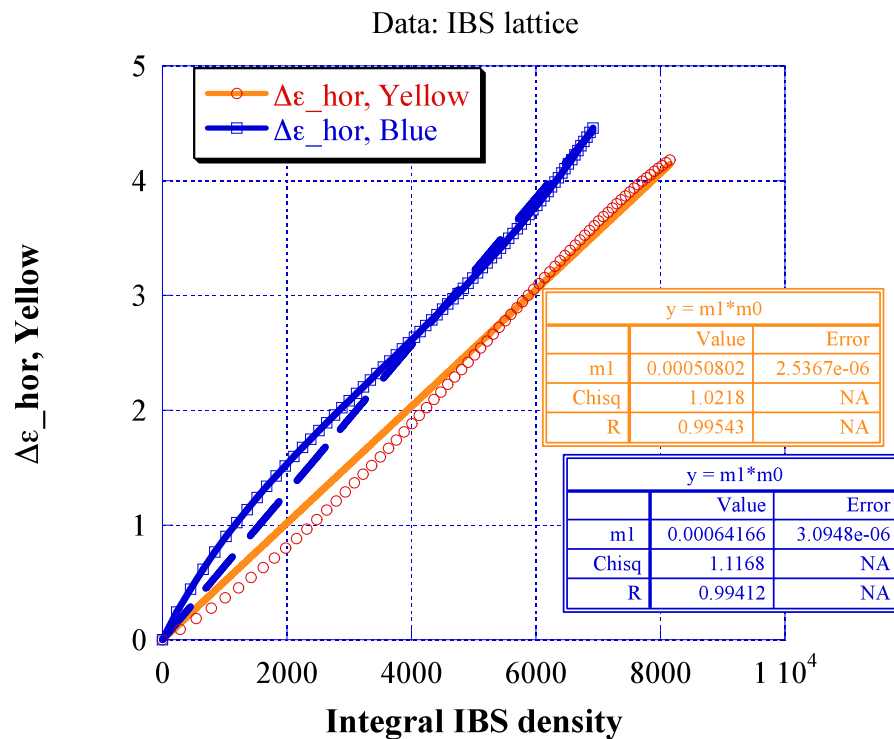
92 deg. phase advance

S. Tepikian

# IBS suppression lattice APEX experiment - June 2007

(V. Litvinenko et al.)

$$IBS \text{ Integral } (t) = \int_0^t \frac{N(t') dt'}{\sigma_z \sqrt{\epsilon_h \epsilon_v} (\epsilon_h + \epsilon_v)}$$



- **Conclusions**
  - Transverse IBS is suppressed by  $30 \pm 10\%$

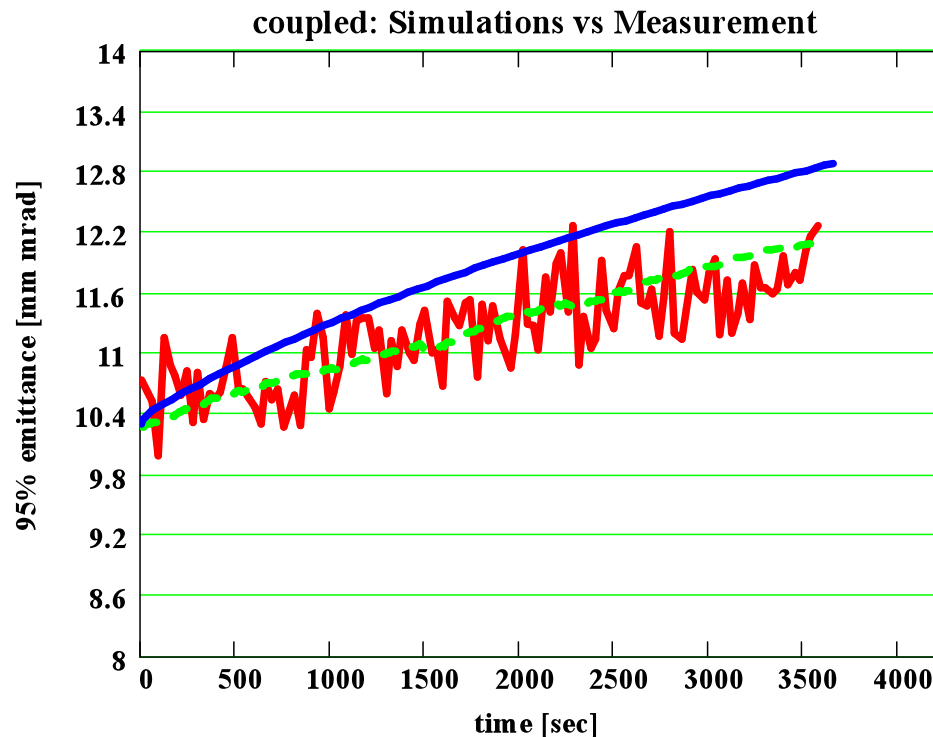
## Coupled case (January 9, 2008 APEX data):

Horizontal emittance growth (simulation vs. measurement, bucket<sup>38</sup> #121)

red – Horizontal emittance (measurement)

blue – expected (simulation) with Run-7 lattice (82 deg./cell)

green – expected (simulation) for Run-8 “IBS-suppression” lattice (92 deg./cell)



Reduction in IBS  
growth rate, as predicted

For simulations  
with 82 and 92 deg.  
lattice, longitudinal  
beam parameters  
(momentum spread and  
bunch length) were  
chosen the same.

# Natural way to compensate IBS diffusions

39

Various cooling techniques:

Radiation cooling

Stochastic cooling

Electron cooling

Laser cooling

Optical stochastic cooling

Coherent electron cooling

***Thank you***